

A NOT operation on Majorana qubits with mobilizable solitons in an extended Su-Schrieffer-Heeger model

YE XIONG¹ and PEIQING TONG^{1,2,3}

¹ *Department of Physics and Institute of Theoretical Physics, Nanjing Normal University, Nanjing 210023, P. R. China*

² *Jiangsu Key Laboratory for Numerical Simulation of Large Scale Complex Systems, Nanjing Normal University, Nanjing 210023, P. R. China*

³ *Kavli Institute for Theoretical Physics China, CAS, Beijing 100190, China*

PACS 73.20.-r – Electron states at surfaces and interfaces
 PACS 73.43.-f – Quantum Hall effects
 PACS 03.65.Vf – Phases: geometric; dynamic or topological
 PACS 71.10.Pm – Fermions in reduced dimensions

Abstract – Coupling Majorana qubits with other qubits is an absolute essential in storing, manipulating and transferring informations for topological quantum computing. We theoretically propose a manner to coupling Majorana qubits with solitons, another kind of topological impurities, which was first studied in the spinless Su-Schrieffer-Heeger (SSH) model. We presents a NOT operation on the Majorana qubit with moving the complementary soliton through heterostructure adiabatically. Based on these two topological impurities, the operation is robust against local disorder. Furthermore, we find that the soliton may carry decimal electric charge instead of fractional charge $1/2$, because of the breaking of gauge invariance induced by superconducting proximity.

Introduction. – Topological phases (TP) of matter are characterized by nontrivial band structures which can not be connected to trivial band structures without closing the band gap at the Fermi energy [1–4]. Due to the holographic principle, symmetry protected boundary states will appear at the boundaries of the system. When the energy gap is opened by superconductivity, the superconductor with nontrivial band structure becomes topological superconductor and Majorana fermions (MFs) may exist at the surfaces. The Z_2 invariant which corresponds to the parity of the number of the MF branches at each boundary can be used to distinguish the superconductive nontrivial TP from the superconductive trivial TP [2, 5, 6]. These MFs are robust against local distortions and are considered to be suitable for physical realization of topological qubit [3]. There are many proposals to generate topological superconductors hosting MFs, based from 1-dimensional (1D) superconducting wires with strong spin-orbital interaction [7, 8] to 2D topological superconductor heterostructures [9, 10] or vortex cores [11].

To realize quantum computing based on Majorana qubits, one needs to transfer quantum informations between different qubits. This is a challenging work because

the nonlocal nature of MFs prohibits local operator to coherently transfer quantum information into and out of topological systems. There are already some proposals to hybridize Majorana qubits with other qubits, for instance, with fluxonium qubit [12], with flux qubit [13], with quantum dot qubit [14] and with superconducting charge qubits [15]. In this paper, we propose to couple the Majorana qubits with soliton qubit, another kind of topological impurities first studied in the spinless Su-Schrieffer-Heeger (SSH) model. These soliton qubits are totally different from the qubits enrolled in the previous proposals. They are topological, localized and mobilizable. In this paper, we find that moving the complementary soliton adiabatically through the SSH region of a heterostructure can induce a NOT operation on the Majorana qubit. This manipulation will operate one kind of topological qubit with another kind of topological qubit. So the operation should be fault tolerant and robust against local disorder.

We start from a 1D extended spinless Su-Schrieffer-Heeger (SSH) model. An effective nearest neighboring p wave superconducting pairing is involved so that the model can be considered as a combination of the SSH model [4, 16] and the Kitaev's toy model [7]. As varying

the parameters, the phases of the model can evolve from TP hosting MFs to another TP hosting solitons. Because the present of superconducting pairing, the electric charge carried by each soliton is no longer universally equal to $1/2$ (in the units $e = 1$). We will raise a topological way to calculate this charge accurately in Sec. 3.

We begin in Sec. 2 by introducing a 1D tight-binding model. This model has three topological nonequivalent phases. We will also illustrate the kinds of topological impurities in these phases. In Sec. 3, we enroll the Thouless pump to the model and calculate the movement of Wannier functions (WFs) during the pump. This can help us find the electric charge carried by each soliton. In Sec. 4, we propose how to apply NOT operation on a Majorana qubit by moving the complementary soliton adiabatically and discuss why local disorder can not affect the operation. In Sec. 5, we emphasis the importance of our findings and discuss new vistas of research in this field.

1D tight-binding model and phase diagram. –

Hamiltonian. We use a Hamiltonian describing 1D spinless dimerized model with the nearest neighboring p wave superconducting coupling,

$$H = \sum_i \{ [1 + (-1)^i \delta] c_i^\dagger c_{i+1} + \text{h.c.} \} + h \sum_i c_i^\dagger c_i + \Delta \sum_i (c_i^\dagger c_{i+1}^\dagger + \text{h.c.}), \quad (1)$$

where c_i^\dagger and c_i are the creation and annihilation operators for electron on site i , respectively, δ is the degree of dimerization, Δ is the strength of p wave pairing, and h is the external global potential. We will only investigate the model with $|\delta| < 1$.

This model could be realized by placing a dimerized polyacetylene on top of an s -wave superconductor. A rotating magnetic field can induce the required giant spin-orbital interaction along the chain [17]. The effective spinless Hamiltonian Eq. (1) is obtained when the Fermi energy lying in the gap opened by the staggered hoppings or by the external magnetic field. Another possible realization of the Hamiltonian has been proposed by Klinovaja *et al.* [18], in which a helical magnetic field plays the role of staggered hoppings.

Phase diagram. The phase boundaries separating different phases in the phase diagram are determined by the fact that the band gap closes there. The Hamiltonian in momentum k reads,

$$H(k) = \{ [(1 - \delta) + (1 + \delta) \cos(k)] \sigma_x + (1 + \delta) \sin(k) \sigma_y + h \sigma_0 \} \otimes \tau_z - \Delta \tau_y \otimes [\sin(k) \sigma_x + (1 - \cos(k)) \sigma_y]$$

The Pauli matrix $\tau_{x,y,z}$ and $\sigma_{x,y,z}$ are operating on particle-hole and sub-lattice subspaces, respectively. σ_0 is a unit matrix. The band gap closes when the parameters obey one of the following two conditions, $\frac{h^2}{4} + \Delta^2 = \delta^2$ (when $|\delta| < 1$) and $h = \pm 2$. In Fig. 1, we sketch out the

first condition with the ellipsoidal cones in the parameter space spanned by h , δ and Δ . Two planes at $h = \pm 2$ (for the second condition) are not showed for the sake of clarity.

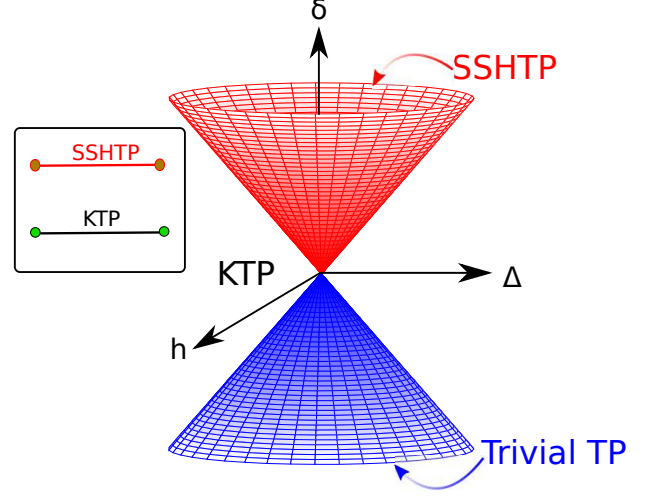


Fig. 1: The phase diagram in the parameter space spanned by δ , Δ and h . The system is in the SSHTP in the region enclosed by the red cone. Within the blue cone and in the region outside two planes $h = \pm 2$ (not showed in the figure), it is in the trivial TP. The system is in the KTP in the rest parameter region. The left inset shows that an open chain in the SSHTP (or in the KTP) can have soliton states (or MFs) as the topological impurities at the ends.

From the phase diagrams for the SSH model and Kitaev's toy model, one can anticipate the topological properties of the TPs in our model. In Fig. 1, for the parameter region enclosed by the red cone, the system is in the TP similar to that of the SSH model. This is because the model can be regressed to the standard SSH model by decreasing both h and Δ to 0 while keeping $\delta > 0$. The band gap at the Fermi energy does not close during this regression. So we call the TP in the red cone as a SSH like TP (SSHTP). For the parameter region in between two ellipsoidal cones and two planes $h = \pm 2$ at distance, the system is in the Kitaev like TP (KTP) because it can be regressed to a standard Kitaev's toy model in TP without closing the band gap. In the left inset of Fig. 1, we schematically show that an open chain in SSHTP (or KTP) can host soliton states (or MFs) at the ends. For the rest regions in the parameter space, including that enclosed by the blue cone and those outside two planes $h = \pm 2$, the system is in the trivial TP. Actually, the trivial phase in these regions can be separately regressed to the trivial TP of the SSH model and to the trivial TP of the Kitaev's toy model, respectively.

Topological impurities appeared at boundaries. To further illustrate the topological nonequivalence of the 3 phases in the phase diagram and show the topological impurities appeared at boundaries, in Fig. 2, we plot the energy spectrum of a ring, in which parameters are ad-

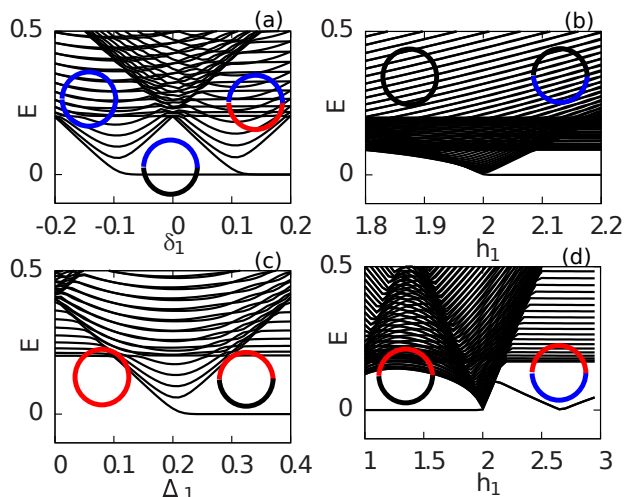


Fig. 2: The energy spectrum of a ring in which the upper half and lower half are in different parameter regions. The length is $N = 400$. The parameters are: (a) $h = 0$, $\Delta = 0.1$ and $\delta = -0.2$ in the upper half and $h = 0$, $\Delta = 0.1$ and $\delta = \delta_1$ in the lower half; (b) $h = 1.8$, $\Delta = 0.1$ and $\delta = 0.2$ in the upper half and $h = h_1$, $\Delta = 0.1$ and $\delta = 0.2$ in the lower half; (c) $h = 0$, $\Delta = 0.1$ and $\delta = 0.2$ in the upper half and $h = 0$, $\Delta = \Delta_1$ and $\delta = 0.2$ in the lower half; (d) $h = 0.6$, $\Delta = 0.1$ and $\delta = 0.4$ in the upper half and $h = h_1$, $\Delta = 0.1$ and $\delta = 0.4$ in the lower half. The phases of the upper and lower parts of the ring are indicated by colors: red for SSHTP, black for KTP and blue for trivial TP.

justed so that the upper and lower parts of the ring are in different phases. The topologically protected boundary states at the joints of two parts should emerge in the energy spectrum with energies inside the band gap. In all panels of Fig. 2, the parameters are fixed in the upper half of the ring, while one of the parameters, referred to δ_1 in (a), h_1 in (b) and (d), and Δ_1 in (c), is varying in the lower half. We indicate types of TPs of the upper and lower parts with different colors: red, black, and blue that represent SSHTP, KTP and trivial TP, respectively. In Fig. 2(a), by varying staggered hoppings δ_1 in the lower half, the ring changes from full trivial TP to half trivial TP and half KTP at $\delta_1 = -0.1$. As a result one zero energy state representing the emergency of two MFs at the joints appears after this transition. When δ_1 is further increased and exceeds $+0.1$, the lower part of the ring enters SSHTP. So in this case, there are two zero energy states inside the band gap that representing the existence of two soliton states. In Fig. 2(b), when $h_1 < 2$ the parts are in the KTP and there is no zero energy state in the gap because there is no boundary between different phases. But when $h_1 > 2$, the phase of the lower half changes to the trivial TP, and we find a zero energy state in the spectrum. These results can be traced back to the well known conclusions in the standard SSH model or in the Kitaev model. Something new happens in the next panels. In Fig. 2(c), the ring is half in the SSHTP and half in the KTP when $\Delta_1 > 0.2$. At each joint, only one MF is left

because the coupling between MF and soliton state at the joint lifts the energy of the soliton state. So there is only one zero energy state left in the gap. In Fig. 2(d), the ring is half in the SSHTP and half in the trivial TP when $h_1 > 2$. This situation is same as that in the right part of Fig. 2(a). But the soliton states in (d) are lifted from zero energy and become Andreev bound states. This Andreev bound states are different from the normal Andreev bound states because they take the responsibility of topological impurities which must appear at the boundaries of different TPs. As a result, as the panel (d) shows, the Andreev bound states can evolves smoothly to zero energy states without closing the band gap.

Because of this topological nature, the evolutions to zero energy states should be robust against disorder. In Fig. 3, disorder is enrolled to the ring by replacing the staggered hopping between the i th and the $(i + 1)$ th site with $1 + (-1)^i \delta + 0.15w$, where w is random numbers distributing uniformly in $[-1, 1]$. Other parameters are the same as those in Fig. 2(d). The figure shows that disorder can remove degeneracies of the Andreev bound states but can *not* destroy them.

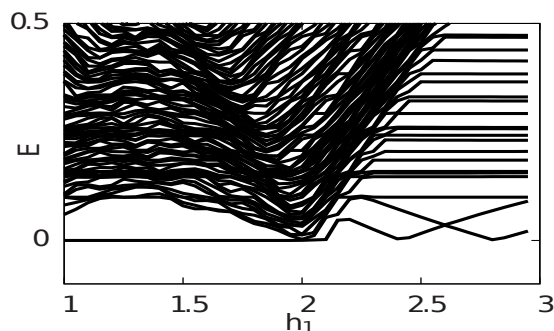


Fig. 3: The energy spectrum of a disordered ring. Most of the parameters are the same as those in Fig. 2(d) except the randomized staggered hoppings $t_i = 1 + (-1)^i \delta + 0.15w$, where w is a random number in $[-1, 1]$.

Thouless pump and decimal charge carried by each soliton. – Similar to that in the standard SSH model, domain walls are mobilizable in the model. To electrically control its movement, the electric charge carried by each domain wall should be determined at the first. In this section, with the help of the evolution of Wannier functions (WFs) during the Thouless pump, we can determine the charge accurately.

Wannier functions for the occupied bands. The most localized WF's for the occupied bands are defined as the eigenvectors of the tilde position operator

$$\tilde{R} = \hat{P} \hat{R} \hat{P}, \quad (2)$$

where \hat{R} is the position operator and \hat{P} is the projection on the occupied states [19–21]. Here \hat{P} can be written explicitly as $\hat{P} = \sum_{\alpha \in \text{occupied states}} |\alpha\rangle \langle \alpha|$ and in the site representation the position operator $\hat{R} = \text{diag}(1, 2, \dots, N) \tau_0$,

where τ_0 is the 2×2 unit matrix in the particle-hole subspace and $\text{diag}(1, 2, \dots, N)$ is a diagonal matrix with the diagonal elements running through lattice sites from 1 to N . The eigenvalues of \tilde{R} , denoted as R s, are the central positions of the WFs. Eq. 2 extends the projected position operator to particle and hole subspaces. As a result, the WFs for the unoccupied bands (from holes), which are absent in the usual particle representation, can be obtained from this new definition. The usual WFs obtained from the traditional definition are plotted in panel (c) in Fig. 4 for comparison.

Thouless pump. The Thouless pump is introduced to the Hamiltonian by varying the staggered hopping and on-site energy slowly with an extra parameter ϕ [4]. Then the Hamiltonian becomes $H(\phi) = \sum_i [1 + (-1)^i \delta \cos(\phi)] c_i^\dagger c_{i+1} + \text{h.c.} + \sum_i (-1)^i h_{\text{st}} \sin(\phi) c_i^\dagger c_i + h \sum_i c_i^\dagger c_i + \Delta \sum_i (c_i^\dagger c_{i+1}^\dagger + \text{h.c.})$.

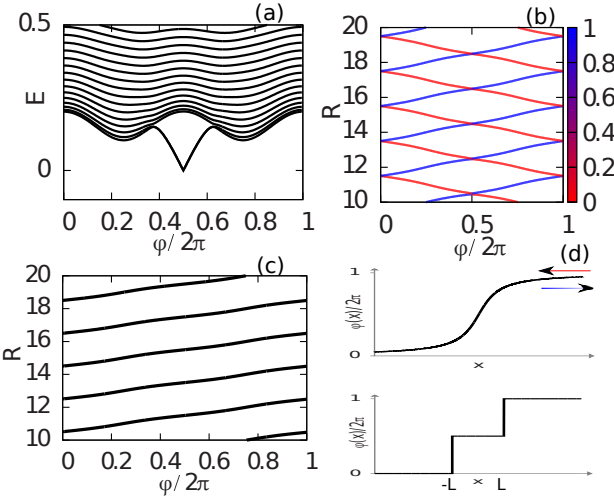


Fig. 4: The energy spectrum (a) and the WFs centers (b) during the Thouless pump of ϕ . The parameters are $h = 0$, $h_{\text{st}} = 0.3$, $\delta = -0.2$ and $\Delta = 0.1$. The colors of the points in panel (b) represent the particle weights of the corresponding WFs in the particle-hole subspace with scale given by the right palette, where 1 (blue) means that the WF contains one particle while 0 (red) indicates that the WF is completely hole like. (c) For comparison, the conventional WFs for a standard SSH model during Thouless pump are showed. (d) A schematic shows the two kinds of layouts of $\phi(x)$ along chains for the arguments in the next subsection.

Evolution of WFs during the Thouless pump. In Fig. 4, we plot the energy spectrum (a) and the centers of WFs (b) as functions of ϕ for a $N = 200$ chain with open boundary condition. The parameters are $h = 0$, $h_{\text{st}} = 0.3$, $\delta = -0.2$ and $\Delta = 0.1$. As Fig. 4(a) shows, the chain is in trivial TP with no boundary state around $\phi = 0$. As ϕ is varying, the chain is pushed to the SSHTP near $\phi = \pi$ and then is pulled back to the trivial TP at the end of a cycle. During this pump, the band gap at the Fermi energy keeps open so that the WFs we calculated are localized and their centers showed in (b) are reliable. As

the model is represented in the Nambu representation, an extra new set of WFs corresponding to the bands of holes emerges. In Fig. 4(b), we use the colors, blue and red to illustrate the weights of the WFs on the particle and hole subspaces, respectively. So blue(red) points in the panel are illustrating that WFs centered at the positions are particle(hole) like functions. Panel (b) shows that the particle like WFs are moving right accompanied with the hole like WFs moving left during the pump.

Electric charge carried by each soliton. For the standard SSH model, there is a counting formula describing the total number M of the unoccupied zero energy states in term of electric charge Q carried by each topological impurity (including both domain wall and geometric end), $M = -2Q \bmod 2$ [22, 23]. The well known fractional charge carried by each soliton is a direct conclusion of this equation (when $M = 1$, $Q = \frac{1}{2}$). Turning on the superconducting coupling will not break the charge conjugation symmetry and the counting formula should survive. But the electric charge Q must be replaced by the conserved quasiparticle charge Q_{BdG} [24] because the global electromagnetic gauge invariance is broken in the BdG mean field Hamiltonian. It should be emphasized that Q_{BdG} is a topological character in the present case and has nothing to do with the actual electric charge \tilde{Q} anymore. So we need to figure out the actual charge \tilde{Q} carried by each soliton in order to electrically control their motion.

We use a thought experiment to figure out the actual electric charge \tilde{Q} as well as the conserved BdG charge Q_{BdG} carried by each soliton. Suppose that there is an infinite chain with Hamiltonian of Eq. (??). The parameter ϕ is not fixed but varying slowly along the chain as $\phi(x)$. The total variation of ϕ along the chain is 2π . Without loss of generality, we let $\phi(-\infty) = 0$ and $\phi(+\infty) = 2\pi$. As $\phi(x)$ is varying slowly (showed in the upper panel in Fig. 4(d)), the positions of WFs for $\phi(x)$ given by Fig. 4(b) are still valid in regions in which $\phi(x)$ changes slightly. Now let's compare the positions of WFs in this chain with those in a uniform chain in which $\phi(x)$ is fixed at 0. At the far left segments of the chains, the positions of WFs in the two chains are the same because $\phi(x) = 0$ in both regions. As increasing x , the WFs are moved slightly away from the positions for the uniform chain because $\phi(x)$ increases. As Fig. 4(b) shows, particle like WFs are misaligned in the x direction accompanied with hole like WFs misaligned in the inverse direction. These deviations keep increasing with x and reach the length of one unit cell in the far right region in which $\phi(x) = 2\pi$. So we conclude that, compared with the uniform chain, the chain with varying $\phi(x)$ loses a particle like WF and gains a hole like WF. This can also be looked as that $\phi(x)$ pushes out a particle like WF and pulls in a hole like WF at the right end of the chain at $x = \infty$. Now we relax the restriction that $\phi(x)$ is varying slowly with x . This relaxation does not alter the above conclusion because the local variation at finite x will not affect physics at ∞ . We choose the new layout of $\phi(x)$ as $\phi(x) = 0$ when

$x < -L$, $\phi(x) = \pi$ when $L > x > -L$ and $\phi(x) = 2\pi$ when $x > L$, where L is a large but finite number (showed in the lower panel in Fig. 4(d)). The new layout is representing a chain with a pair of domain wall and anti-domain wall at $\pm L$. We know that each domain wall (anti-domain wall) has a soliton state on it. So these two soliton states must take the responsibility of the lost and gained WFs. As a result, each soliton takes half of the total lost charges, $\tilde{Q} = -\frac{1}{2}[\langle \Psi_{\text{Particle like WF}} | \hat{\rho} | \Psi_{\text{Particle like WF}} \rangle - \langle \Psi_{\text{Hole like WF}} | \hat{\rho} | \Psi_{\text{Hole like WF}} \rangle]$, where $\hat{\rho}$ is the single particle density operator $\hat{\rho} = \sum_i c_i^\dagger c_i$ and $|\Psi_{\text{Particle(Hole) like WF}}\rangle$ is a wave function of the particle(hole) like WF. For a chain with the parameters showed in Fig. 4(a) and (b), this charge \tilde{Q} is still $\frac{1}{2}$. As to the conserved BdG charge Q_{BdG} , this conserved charge counts that how many WFs have been pushed out from the chain with one domain wall. From the above argument, we see it is universal $\frac{1}{2}$.

We have calculated the energy spectrum as well as the motions of WFs during the Thouless pump for a chain with nonzero external potential, $h = 0.3$, for comparison. Other parameters are same as those in Fig. 4. We find that h lifts the energies of the soliton states at $\phi = \pi$ but the motions of WFs are same as those showed with $h = 0$. But these WFs have been altered from pure particle like or hole like functions to mixed functions. We can count the total charge being pump out and find that it is 0.97 instead of 1. As a result, each soliton in this model carries decimal charge 0.485. So we can conclude that the charge carried by each soliton is **not** a universal fractional number but depends on h when $h \neq 0$.

Manipulating Majorana qubit by moving soliton.

– In the present model, there are two kinds of topological impurities, solitons and MFs. We will show that when coupling these two kinds of topological impurities together, we can change the state of Majorana qubit by adiabatically moving the complementary soliton along the chain. In the following, we are concentrating on the two MFs taking part in the coupling and ignoring the two uncoupling MFs at the other far ends.

The heterostructure. As the inset in Fig. 5(a) shows, a circular polyacetylene is placed on the surface of a nonuniform superconductor so that one part of the circle is in the KTP (the black arc) and the rest is in the SSH phase (the red arc). We suppose that there is a domain wall (sketched by the blue point) in the circle. In our numerical calculation, this domain wall is simulated by two adjacent stronger bonds with hoppings $t + \delta$. It will induce a soliton state when the domain wall is in the SSH region. It should be noted that because the existence of domain wall the total length of circle is an odd number instead of even ones. There are two MFs (indicated by the green points) at the joints of the arcs.

Fig. 5(a) shows the energy levels of the ring as the domain wall is moved adiabatically. The domain wall starts from where it is showed in the inset. When it is in the

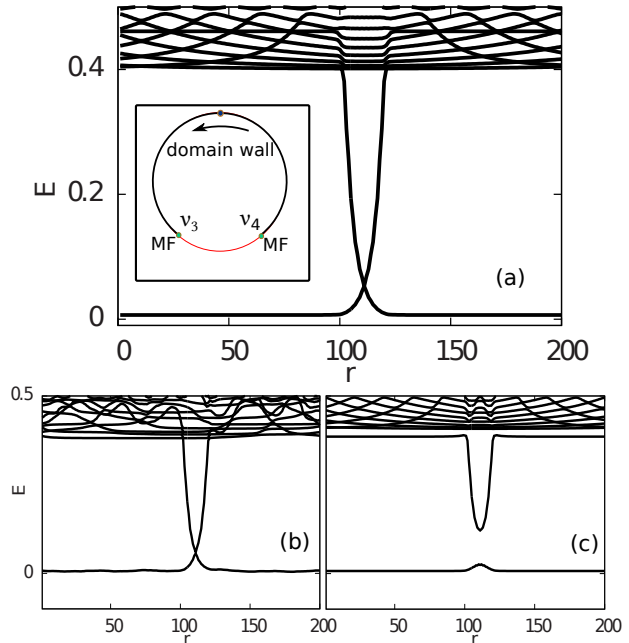


Fig. 5: (a) The energy spectrum of the heterostructure ring, showed in the inset, when the domain wall (blue point) is moving. The length of the ring which hosts the domain wall is $N = 201$. One part of the ring is in the KTP (black) and the rest is in the SSH phase (red). MFs appearing at the joints are indicated by the green points. The parameters are $h = 0$, $\delta = 0.2$, $\Delta = 0$ for the part in the SSH phase and $h = 0$, $\delta = 0.2$, $\Delta = 0.4$ for the other part. The length of the SSH region is 20. (b) The robust level cross for a disordered chain. The parameters are same as those in (a) except the randomized staggered hopping. (c) The level crossing becomes anti-crossed when $h = 0.1$.

black arc in the KTP, there is only one zero energy state referring to the two MFs because domain wall in the KTP region can not induce soliton state inside the band gap [25]. Soliton state will appear in the gap and its energy is decreasing when the domain wall is moved into the SSH region, while the zero energy state is lift up in energy. These two energy levels cross when the domain wall is passing the center of the SSH region. Because of this level crossing, particle occupations on the zero energy state and on the soliton state will exchange after passing the wall through the SSH region adiabatically. This mechanism can modify the Majorana zero energy state with a complementary soliton, say $n_f^{ZE} = n_i^s$ and $n_f^s = n_i^{ZE}$, where $n_{i(f)}^{ZE(s)}$ is number of particle on the MF zero energy (soliton) state before(after) the movement of domain wall.

The above level crossing implies a mechanism to manipulating MF qubits by moving soliton. A MF qubit need four MFs. Let's denote their MF operators as μ_1, μ_2, μ_3 and μ_4 . The heterostructure is extended from that has been discussed in Fig. 6 with the SSH region (red) and the KTP region (black). The four MFs are illustrated by 1, 2, 3 and 4 in the figure. Our discussion is in fermion representation with the complex fermion creation operator

$\psi_\beta^\dagger = (\mu_1 + i\mu_2)/2$ and $\psi_\alpha^\dagger = (\mu_3 + i\mu_4)/2$. The quantum states of the MF qubit are illustrated as $|n_\alpha n_\beta\rangle$, where n_α and n_β can take 0 (empty) and 1 (occupied). Traditionally, the two states of a MF qubit are defined as "0" state: $|10\rangle$ and "1" state: $|01\rangle$.

We can extend the above notation of quantum states to include the occupation on the soliton state as $|n_\alpha n_\beta, n_{soliton}\rangle$. The states showed in the figure are in this extended form. Now we show explicitly how NOT operation works. Supposing the initial state is $|01, 0\rangle$ with the domain wall at the "3" o'clock direction. After moving the it to the "9" o'clock direction, n_β and $n_{soliton}$ exchange due to the level crossing. So we get the state $|00, 1\rangle$. After moving the domain-wall a circle back to the "3" o'clock direction. n_α and $n_{soliton}$ exchange and we get $|10, 0\rangle$. Finally the domain-wall is moved an extra one half circle to the "9" o'clock direction. The state keeps at $|10, 0\rangle$. This is a NOT operation that changes from "1" state to "0" state for MF qubit. In the next three rows in the figure, we show explicitly that this NOT operation is independent on the initial state of $n_{soliton}$ and works well for the case, "0" to "1".

The only mechanism that will introduce fault to the NOT operation is that the quasi-particle on soliton state may spontaneously jump to the zero energy state when the zero energy state is empty. But thanks to the localization nature of zero energy state (localized at two positions of MFs) and soliton state, this possibility is in the scale of $1/L$ in most case, where L is the length of the KTP region.

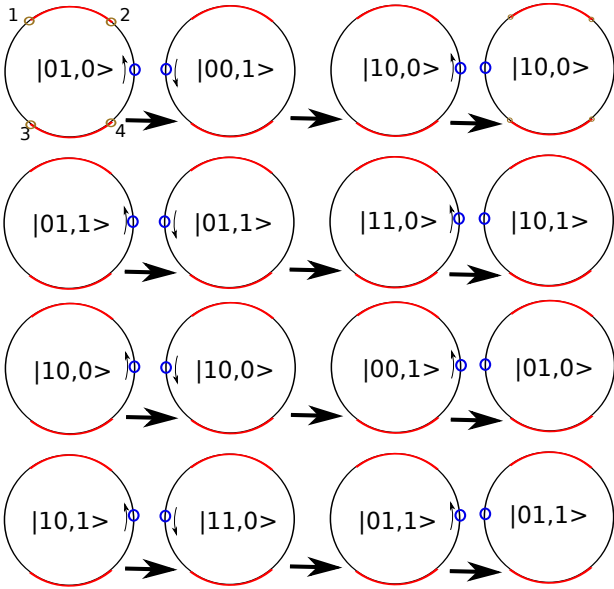


Fig. 6: How NOT operation works for a MF qubit. The red region is in the SSH phase and the black region is in the KTP. The domain-wall is the blue point. The quantum state in each case is written at the center of each circle.

Robust level crossing against disorder. This NOT operation on Majorana qubit depends crucially on the fact that the level crossing must be robust against disorder

or must be protected. In Fig. 5(b), we plot the energy spectrum for a disordered ring. The parameters are the same as those in (a) except that the staggered hoppings are randomized, $t_i = 1 + (-1)^i \delta + 0.1w$, where w is a random number in $[-1, 1]$. This figure shows that the level crossing is reserved even when this huge disorder is introduced. In Fig. 5(c), we show that the level crossing can be destroyed by a nonzero external potential h . The parameters are same as those in (a) except $h = 0.1$.

The above crossing and anti-crossing effects can be understood by expressing the effective Hamiltonian for the low energy states (inside the band gap) in the Majorana representation. The MFs at the joints are denoted by ν_3 and ν_4 and the soliton state is regraded as a combination of two MFs, denoted by ν_1 and ν_2 . For the effected Hamiltonian spanned by these 4 Majorana states, the coupling between ν_1 and ν_2 is proportional to the energy of the soliton state E_s , while the coupling between ν_1 and ν_3 (or ν_2 and ν_4) is proportional to $e^{-\alpha d_{13}}$ (or $e^{-\alpha d_{24}}$), where α is proportional to the band gap of the SSH phase and d_{13} (or d_{24}) is the distance between the MFs ν_1 and ν_3 (or ν_2 and ν_4). When $h = 0$ and the domain wall is moved deeply to the SSH region, the finite size effect can only lift up the energy of the soliton state by $e^{-\alpha L}$, where L is the length of the SSH region. This is much smaller than the coupling between ν_1 and ν_3 (ν_2 and ν_4) because d_{13} and d_{24} are in the scale of $\frac{L}{2}$. So the level crossing must be protected by the leading couplings in the effective Hamiltonian. But when $h \neq 0$, the energy of the soliton state in the SSH region is nonzero intrinsically and the coupling between ν_1 and ν_2 must be considered. So the crossing is not protected anymore.

The above manipulation on Majorana qubit is a complementary operator to the braiding operators. For a system with $2n$ MFs, exchanging MFs will introduce a non-Abelian unitary transformation in the Hilbert space spanned by the degenerated ground states. But because the braiding operators conserve the parity of the number of fermions, they should operate in two independent 2^{n-1} dimensional sub-spaces (corresponding to even and odd parities, respectively) [26]. By enrolling the NOT operator we just mentioned, quantum computing can take the benefits of the whole Hilbert space with the dimension 2^n , instead of only half of it.

Discussions. — We propose a NOT operation on Majorana qubits through adiabatically moving the complementary soliton. The two ingredients of the operation are both topological impurities so that local disorder can not influence it. Compared with the other proposals, our proposal is more ascendant on flexibility and scalability. For instance, the mechanism can be extended to a network hosting multiple Majorana qubits. One can apply the operation on the desired qubits subsequently by moving a soliton in this network.

* * *

The work was supported by the State Key Program for Basic Research of China (Grant Nos. 2009CB929504, 2009CB929501), National Foundation of Natural Science in China Grant Nos. 10704040, 11175087.

REFERENCES

- [1] QI X.-L. and ZHANG S.-C., *Rev. Mod. Phys.*, **83** (2011) 1057.
- [2] HASAN M. Z. and KANE C. L., *Rev. Mod. Phys.*, **82** (2010) 3045.
- [3] NAYAK C., SIMON S. H., STERN A., FREEDMAN M. and DAS SARMA S., *Rev. Mod. Phys.*, **80** (2008) 1083.
- [4] SHEN S.-Q., *Topological Insulators, Dirac Equation in Condensed Matters* (Springer Series in Solid-State Science 174) 2012.
- [5] KANE C. L. and MELE E. J., *Phys. Rev. Lett.*, **95** (2005) 146802.
- [6] MOORE J. E. and BALENTS L., *Phys. Rev. B*, **75** (2007) 121306.
- [7] KITAEV A. Y., *Phys. Usp.*, **44** (2001) 131.
- [8] LUTCHYN R. M., SAU J. D. and DAS SARMA S., *Phys. Rev. Lett.*, **105** (2010) 077001.
- [9] FU L. and KANE C. L., *Phys. Rev. Lett.*, **100** (2008) 096407.
- [10] ALICEA J., *Phys. Rev. B*, **81** (2010) 125318.
- [11] SATO M. and FUJIMOTO S., *Phys. Rev. B*, **79** (2009) 094504.
- [12] PEKKER D., HOU C.-Y., MANUCHARYAN V. E. and DEMLER E., *Phys. Rev. Lett.*, **111** (2013) 107007.
- [13] JIANG L., KANE C. L. and PRESKILL J., *Phys. Rev. Lett.*, **106** (2011) 130504.
- [14] BONDERSON P. and LUTCHYN R. M., *Phys. Rev. Lett.*, **106** (2011) 130505.
- [15] HASSLER F., AKHMEROV A. R. and BEENAKKER C. W. J., *New. J. Phys.*, **13** (2011) 095004.
- [16] SU W. P., SCHRIEFFER J. R. and HEEGER A. J., *Phys. Rev. Lett.*, **42** (1979) 1698.
- [17] KLINOVAJA J. and LOSS D., *Phys. Rev. X*, **3** (2013) 011008.
- [18] KLINOVAJA J., STANO P. and LOSS D., *Phys. Rev. Lett.*, **109** (2012) 236801.
- [19] THOULESS D., *J. Phys. C*, **17** (1984) L325.
- [20] THONHAUSER T. and VANDERBILT D., *Phys. Rev. B*, **74** (2006) 235111.
- [21] QI X.-L., *Phys. Rev. Lett.*, **107** (2011) 126803.
- [22] SU W. P. and SCHRIEFFER J. R., *Phys. Rev. Lett.*, **46** (1981) 738.
- [23] JACKIW R. and SCHRIEFFER J., *Nuclear Physics B*, **190** (1981) 253 .
- [24] SANTOS L., NISHIDA Y., CHAMON C. and MUDRY C., *Phys. Rev. B*, **83** (2011) 104522.
- [25] *When we use soliton state to mention the domain wall, the wall is in the ssh region by default.*
- [26] IVANOV D. A., *Phys. Rev. Lett.*, **86** (2001) 268.